Transmittivity of 2D graded phononic crystals in the frequency and time domains

Olivier Lenoir, Kun Zong, Hervé Franklin, Mihai Predoï

Transmittivity of 2D graded phononic crystals in the frequency and time domains

O. Lenoir[a], K. Zong[a], H. Franklin[b] and M. Predoï[a]

[a]Laboratoire Ondes et Milieux Complexes, Université du Havre, Place R. Schuman, 76610 Le Havre, France
[b]LOMC, CNRS UMR 6294, Université Le Havre, 25, rue Philippe Lebon, 76600 Le Havre, France
olivier.lenoir@univ-lehavre.fr

The media of interest are composed of N parallel infinite rows of steel cylindrical shells, periodically spaced, immersed in water. The influences of geometrical perturbations from rows to rows are investigated. Either the inner radius of the shells between two adjacent rows is varied, or the spacing between the rows is changed. The steel rows can also be replaced by steel-polyethylene bilayers. Time domain simulations have been performed using COMSOL® to visualize the spread of wave packets in the structures. In the frequency domain, the stop bands and pass bands of the transmission coefficient in the different cases are compared. The perturbations cause either the appearing of narrow pass bands in the stop bands, or the widening of the stop bands. If a harmonic plane wave is normally incident on an infinite row, we highlight the transmission (resp. the total reflection) of the waves by the phononic crystal for certain frequencies located in pass bands (resp. stop bands). If the incident wave is sent normally to the N rows, deviations or focalizations of the transmitted waves with respect to the incident direction are observed.

1 Introduction

We investigate the effects of periodicity perturbations in phononic crystals composed of N parallel rows of identical steel shells immersed in water. These perturbations include variations of the inner radius of shells, of the spacing between rows and of the number of rows forming the phononic crystal (PC). We focus particularly on the effects of those periodicity perturbations on the pass bands and stop bands appearing in the plot of the transmission coefficient versus reduced frequency. The steel rows can be replaced by steel-polyethylene bilayers. In this case, the same types of geometrical perturbations are studied in the frequency domain. Simulations in the time domain, when an incident wave is sent normally to the N rows are also performed. Two configurations are investigated. Either the thickness of the tubes are increased from the bounds of the crystal to its middle, or conversely, giving rise to focalizations or deviations of the transmitted waves.

2 Stop bands and pass bands of a steel shell phononic crystal

The geometry of the PC is given in Figure 1. The structure is immersed in water (density ρ_w = 1000kg/m^3, sound velocity c_w=1470m/s). Each row contains an infinite number of steel shells parallely and periodically spaced along the Y direction with a spacing d. For steel, the density is ρ_s = 7900kg/m^3, the longitudinal and transverse velocities are c_l=5790m/s and c_t=3100m/s. The relative thickness of one shell is fixed by the ratio b/a=0.88 where a and b denote the outer and the inner radius of the shell (a=5mm). The spacing d is equal to 2.65a. We consider a PC made up of N regularly spaced identical rows along the X direction, with a spacing D (D/a=3) from centre to centre. The incident wave is a plane harmonic pressure wave whose expression is given by

$$p(x,t) = A\sin(kx - 2\pi f_0 t)\, e^{-20(t-t_0)^2/dt^2},$$

with A=10^6 Pa, $t_0=\alpha/f_0$ and $dt=\beta/f_0$ and (α =2 and β =6). This wave propagates in the X direction and is normally incident on the PC as indicated in Figure 1.

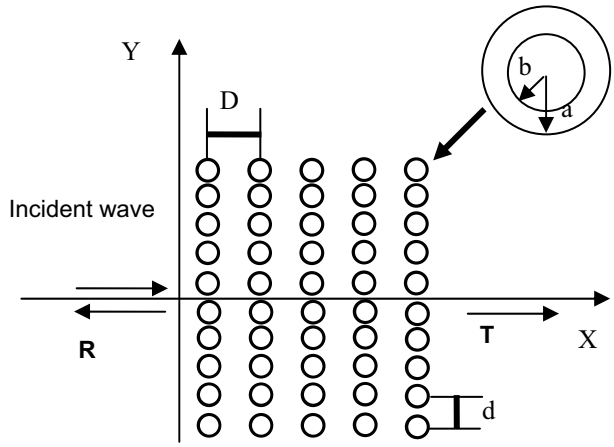

Figure 1: Geometry of steel phononic crystal.

The transmission coefficient T is obtained using both the multiple scattering method in a row [1] and Fabry Pérot method between adjacent rows [2-4]. Figure 2 shows the modulus of this transmission coefficient plotted versus reduced frequency ka, where $k=2\pi f_0/c_w$ (N=14 rows). A large stop band can be observed in the reduced frequency interval 0.8-1.4 while on both sides, undulations appear in the pass bands. The number of oscillations increases with the number of rows. Results on PCs made up of steel shells were obtained also by Khelif *et al.* [5] by using a FDTD calculation.

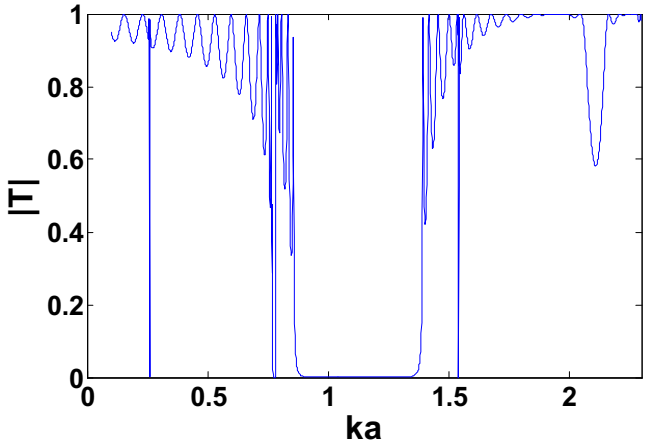

Figure 2: Transmission coefficient for 14 rows

We give below the results of simulations for two values of ka, at a given time. In this work, absorbing conditions are applied at the boundaries of the boxes containing the PC, except the side of the incident wave. When the reduced frequency ka lies in a stop band we have the situation of Figure 3(a) where the wave fronts are

reflected. The waves propagating in the PC are strongly attenuated and no transmitted waves can be observed. The waves do not penetrate the PC more than on its half length. When the reduced frequency ka takes values in a pass band, the incident wave travels through the PC : a total transmission of the wave is observed (no reflection occurs). The waves propagate in the PC with very little attenuation. The maximum of the pressure field corresponds to the red color (10^6 Pa) and the minimum to the blue color (-10^6 Pa).

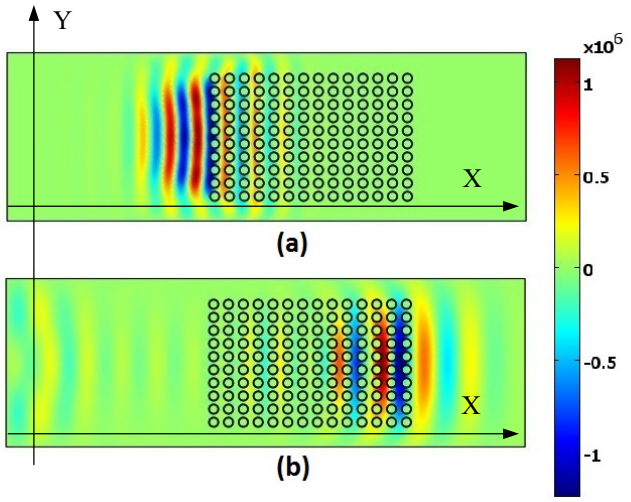

Figure 3: (a) Simulation at t=215µs, ka=1.1 (stop band); (b) Simulation at t=365µs, ka=0.714 (pass band).

3 Engineering stop bands with particular PCs

3.1 PCs with regularly spaced bilayers

Let us consider now PCs composed of a sequence of N bilayers. A bilayer is made up of one row of steel shell and one row of polyethylene shell, with b/a = 0.88, d/a = 2.65 and D/a =3 [6]. Polyethylene has density ρ_P=940 kg/m^3, the longitudinal and transverse velocities are c_l=2370 m/s and c_t=800 m/s. We consider at first the case where the bilayers are separated by a constant spacing D, as shown in Figure 4.

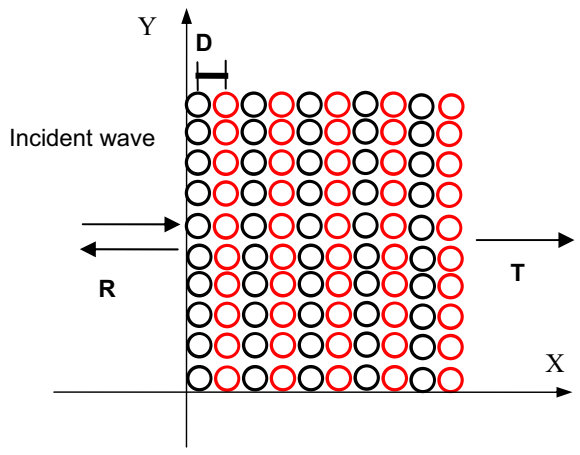

Figure 4: Geometry of steel-polyethylene bilayers (D/a = 3)

The transmission coefficients for 10 and 100 bilayers are presented in Figure 5.

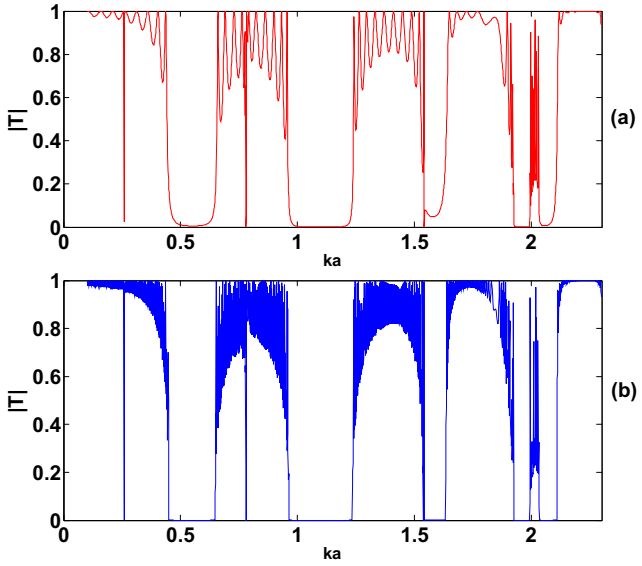

Figure 5: (a) Transmission coefficient for 10 bilayers; (b) Transmission coefficient for 100 bilayers.

In the cases (a) and (b), five stop bands are observed. They are more marked for 100 bilayers (Figure 5(b)) than for 10 bilayers (Figure 5(a)). The width of the stop bands are nearly the same. The number of oscillations in the pass bands between two stop bands is linked with the number of bilayers. The first three stop bands are associated to the steel rows and the two last ones to polyethylene rows. Simulations in the time domain give similar results to those shown in Figures 3(a) and 3(b). It is to be noted that for d/a= 2.3 the pass band around ka = 2 disappears.

3.2 PCs with varied spacing between bilayers

We now consider an increasing spacing between the bilayers in the X direction., as sketched in Figure 6. The variation of spacing between adjacent bilayers obeys the law D_N= (3+0.1(N-1))a.

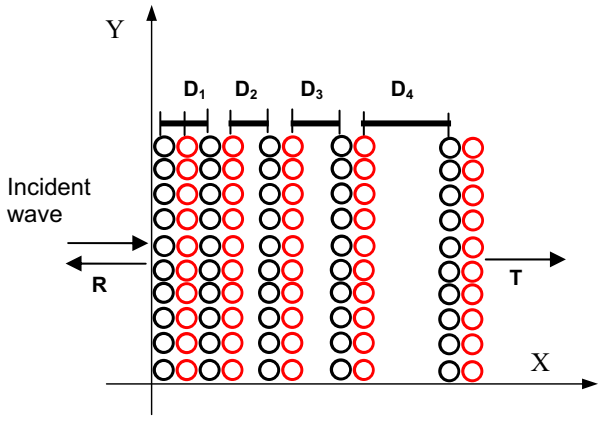

Figure 6: Geometry of steel-polyethylene bilayers with a variation of spacing.

The transmission coefficient for 10 and 100 bilayers are shown in Figure 7. For 10 bilayers (Figure 7(a)), the transmission coefficient presents few differences with the one of Figure 5(a), except at high frequency, around ka=2 where a larger band gap takes place.

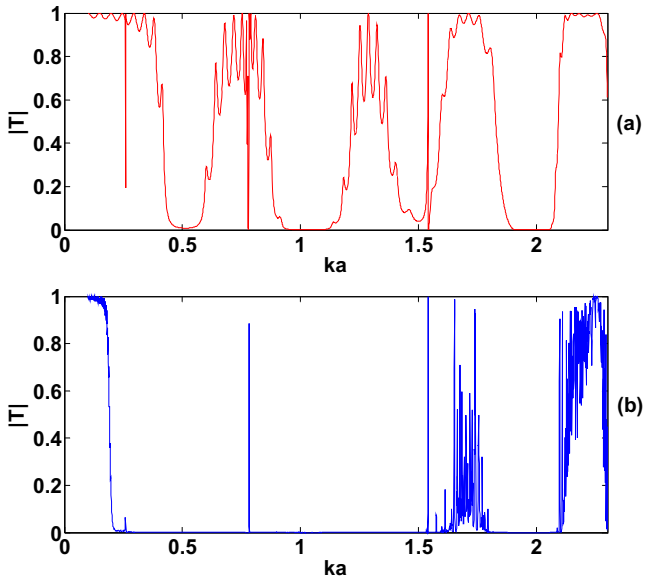

Figure 7: (a) Transmission coefficient for 10 bilayers; (b) Transmission coefficient for 100 bilayers.

For 100 bilayers (Figure 7(b)), the transmission coefficient is completely different of the one shown in Figure 5(b). A very large stop band is now observed between ka = 0.2 and ka = 1.5, whereas two pass bands exist in the case of a regular spacing. For the chosen value of d/a, it still exists a pass band in the normalized frequency range 1.6-1.8. It can be shown that for d/a = 2.3 the pass band located in the interval of ka 1.6-1.8 disappears, so the stop band is even more widened. This objective of finding large band gaps can be encountered in the case of PCs made up of cylindrical air inclusions in an elastic host matrix [7].

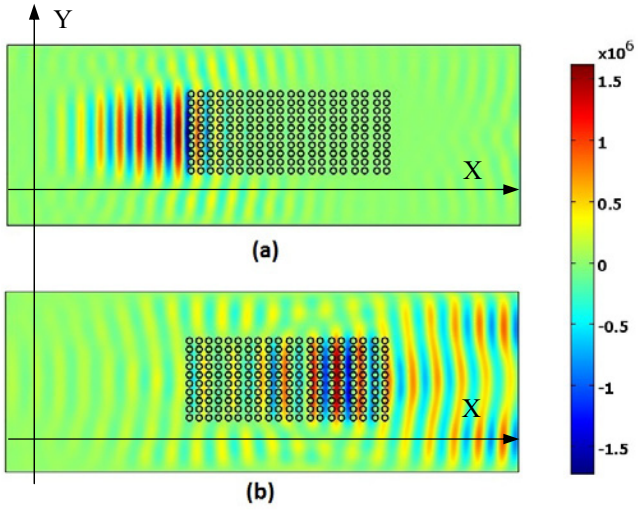

Figure 8: Simulation at t = 800µs (a), ka = 1 (stop band); (b) ka = 0.81 (pass band).

Figures 8(a) and 8(b) show simulations in time domain in the case of 10 bilayers, for two frequencies, ka = 1 (stop band) and ka = 0.81 (pass band), chosen in Figure 7(a). The values of the parameters α and β in the incident pressure wave are 8 and 24, respectively. In the case (a), the incident wave is reflected by the PC without any transmission, whereas in case (b), it is transmitted through it, without any reflection.

4 Focalization

Let us consider a PC composed of 12 rows of steel shells parallel to the Y axis as shown in Figure 9. From the outer row to the central row, the thickness of the shells increases while the spacing between rows decreases. The ratio b/a is varied from 0.9 to 0.4 by step of - 0.1. The spacing law is D_N= (3-0.4(N-1))a. So the density of the matter increases from the exterior to the interior of the structure. No simple analytical expression of the transmission coefficient can be obtained in the case where the wave impinges the structure as shown in the figure. Only simulations in the time domain were performed using COMSOL®.

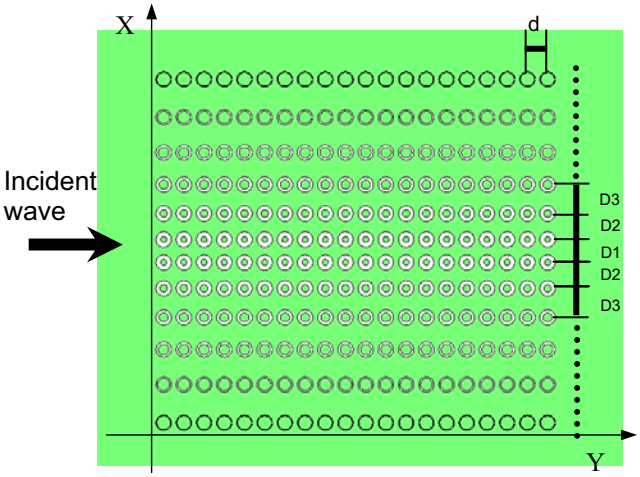

Figure 9: Geometry of a PC for simulating the focalization.

Let us select the values ka = 0.85, α =2 and β =4. As shown in Figure 10, the wave is transmitted by the PC. This process is accompanied by a deformation of the wave fronts and at the time t = 380µs, a focalization of the wave occurs.

Similar results, but for a denser packed set of cylinders have been shown in Ref. [8]. The focalization is due to the variation of the density of shells in the PC. The wave converges towards the symmetry line of the PC corresponding to the place of higher matter density. Such a structure can be seen as an acoustic lens. The location of focalization can be modified by varying the length of the rows in the Y direction. According to the shell thickness and to the row spacing variations, the size of the focal spot can be settled.

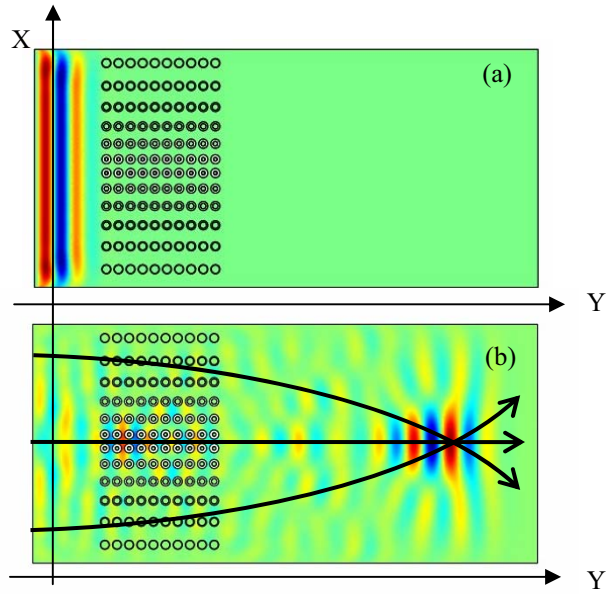

Figure 10: Simulation of the focalization at t = 64µs (a) and at t = 380µs (b) for ka = 0.85. The rays indicate the focalization point.

5 Deviation

A configuration in which the thickness of the shells decreases from the exterior to the interior of the PC is now examined. The b/a ratio range from 0.4 to 0.9 by step of 0.1. The law of variation of the spacing between rows of section 4 is kept. The geometry of such a PC is given in Figure 11. We still consider an incident wave in the Y direction.

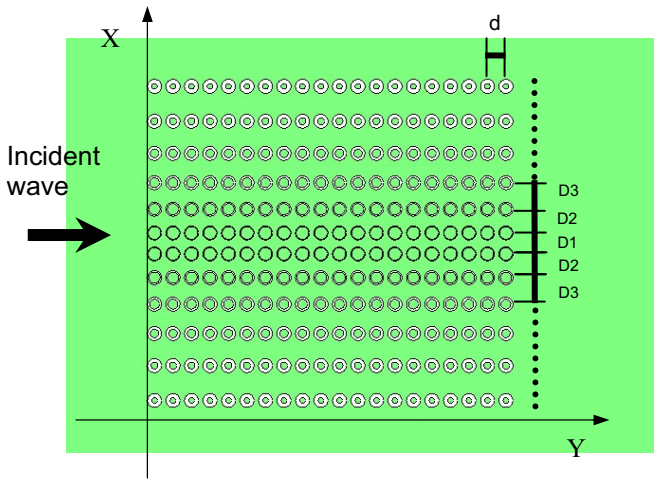

Figure 11: geometry of a PC for simulating deviations.

For the same values of ka, α and β as in section 4, the incident wave propagates through the PC. As shown in Figure 12, the initial wave splits into two ones. Each of these waves deviates towards the regions of high matter density. At the time t = 560µs, they are located in symmetrical directions with respect to the symmetry line of the PC.

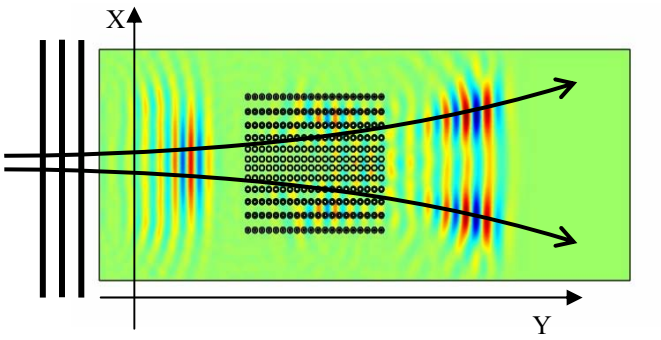

Figure 12: Simulation of the deviation at t = 560µs for ka = 0.85, showing the reflected wave, the splitting of the transmitted wave and the trajectories.

6 Deviation and rebuilding

In this section, our purpose is to obtain a perfect split of the incident wave behind in the outer side of the PC allowing to isolate a domain not (or very slightly) perturbed by the wave. It will be interesting in this context to rebuild the initial wave by setting at an adequate distance one focalizing PC of the type of those studied in section 4.

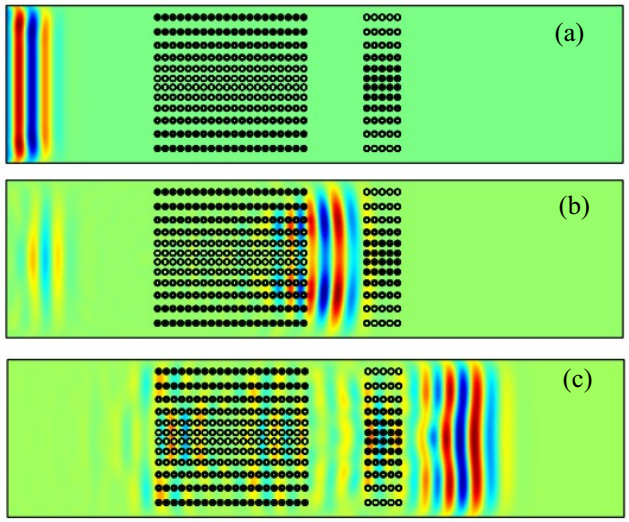

Figure 13 Simulation of the deviation and its rebuilding, at t=90µs (a), t= 471µs (b) and t= 636µs (c) for ka=0.64

As shown in Figure 13, we send a plane wave to the PC (a) which has the same geometry than the ones studied in section 5, and then the initial wave splits into two ones (b).We chose 20 rows of deviating PC in order for the incident wave to be relatively well separated into two waves. For the same reason, we fix the distance between the two types of PCs is equal to 0.108m. After, the two waves cross the second part of the whole structure containing 5 rows of focalizing PC, One recovers almost the same form as the incident wave (c). If we take more rows, the wave is focalized.

7 Conclusion

Various configurations of PCs composed of elastic shells have been studied in the frequency and time domains in this work. Its aim was to analyze the influence of periodicity perturbations on the stop bands and pass bands of the transmission spectra on the one hand, and on the type of propagation through a given PC on the other hand.

It is shown for PCs composed of N regularly spaced infinite rows of identical shells that the transmission coefficient exhibits pass bands and stop bands. The transmission spectrum is calculated by using the multiple scattering theory and a Debye series expansion when the incident wave is sent normally to the infinite rows. The number of undulations in the pass bands depends on the number of rows. The more important this number is, the more marked the stop bands are.

If we replace regularly spaced steel rows by steel-polyethylene bilayers, the transmission spectrum can be largely modified. We can also consider a PC composed of N irregularly spaced bilayers. Widenings of stop bands are observed in comparison to the previous case. When both variations of thickness and row spacing are taken into account, focalization or deviation phenomena are put in evidence, under certain conditions of insonification : the propagation direction of the incident wave is normal to the finite side of the PC. Finally, with these results, we can create structures associating deviating and focalizing PCs in order to rebuild the incident wave.

The possible perspectives will be to consider oblique incidence and to obtain spectra in the cases of focalization and deviation.

References

[1] V. Twersky, " On the scattering of waves by an infinite grating ", IEEE Transactions on Antennas and Propagation **AP-4** 330-345 (1956).

[2] X. Y. Huang, M. A. Heckl, "Transmission and dissipation of sound waves in tube bundles ", Acustica **78**, 191-200 (1993)

[3] R. Sainidou, N. Stefanou, I. E. Psarobas, A. Modinos, " A layer-multiple scattering method for phononic crystals and heterostructures of such ", Comp. Phys. Commun. **166**, 197-240 (2005)

[4] P. M. Martin, Multiple scattering: interaction of time-harmonic waves with N obstacles, Cambridge University Press, 2006.

[5] A. Khelif, P. A Deymier, B. Djafari-Rouhani, J. O. Vasseur, L. Dobrzynski, " Two-dimensional phononic crystal with tunable narrow pass-band: Application to a waveguide with selective frequency ", J. Appl. Phys. **94** (3), 1308-1311 (2003).

[6] K. Zong, H. Franklin, O. Lenoir " Etude de cristaux phononiques de N périodes d'un bi-réseau de cylindres infinis " 10ème Congrès Français d'Acoustique, Lyon, 12-16 Avril 2010

[7] Yun Lai, Zhao-Qing Zhang, " Large band gaps in elastic phononic crystals with air inclusions ", Appl. Phys. Lett. **83** (19), 3900-3902 (2003)

[8] A. Climente, D. Torrent, J. Sanchez-Dehesa, " Sound focusing by gradient index sonic lenses ", Appl. Phys. Lett. 104103 (2010).